Kinetics and Mechanism of Oxidation of *N*, *N*′-Dimethylaminoiminomethanesulfinic Acid by Acidic Bromate

Adenike A. Otoikhian and Reuben H. Simoyi*

Department of Chemistry, Portland State University, Portland, Oregon 97207-0751

Received: March 21, 2008; Revised Manuscript Received: May 8, 2008

The major metabolites of the physiologically active compound dimethylthiourea (DMTU), dimethylaminoiminomethansesulfinic acid (DMAIMSA), and dimethylaminoiminomethanesulfonic acid (DMAIMSOA) were synthesized, and their kinetics and mechanisms of oxidation by acidic bromate and aqueous bromine was determined. The oxidation of DMAIMSA is much more facile and rapid as compared to a comparable oxidation by the same reagents of the parent compound, DMTU. The stoichiometry of the bromate−DMAIMSA reaction was determined to be $2BrO_3^- + 3NHCH_3(=NCH_3)CSO_2H + 3H_2O \rightarrow 3SO_4^{2-} + 2Br^- + 3CO(NHCH_3)_2 + 6H^+$, with quantitative formation of sulfate. In excess bromate conditions, the stoichiometry was $4BrO_3^- + 5NHCH_3(=NCH_3)CSO_2H + 3H_2O \rightarrow 5SO_4^{2-} + 2Br_2 + 5CO(NHCH_3)_2 + 6H^+$. The direct bromine−DMAIMSA reaction gave an expected stoichiometric ratio of 2:1 with no further oxidation of product dimethylurea (DMU) by aqueous bromine. The bromine−DMAIMSA reaction was so fast that it was close to diffusion-controlled. Excess bromate conditions delivered a clock reaction behavior with the formation of bromine after an initial quiescent period. DMAIMSOA, on the other hand, was extremely inert to further oxidation in the acidic conditions used for this study. Rate of consumption of DMAIMSA showed a sigmoidal autocatalytic decay. The postulated mechanism involves an initial autocatalytic build-up of bromide that fuels the formation of the reactive oxidizing species $HBrO_2$ and HOBr through standard oxybromine reactions. The long and weak C−S bond in DMAIMSA ensures that its oxidation goes directly to DMU and sulfate, bypassing inert DMAIMSOA.

Introduction

N, *N*′-Dimethylaminoiminomethanesulfinic acid (DMAIMSA) is one of the more stable metabolites formed in the metabolic activation of dimethylthiourea (DMTU) via an S-oxygenation pathway.[1–3] DMAIMSA exists as a zwitterionic species in its solid form, with positive charges delocalized around its sp^2-hybridized carbon center and two nitrogen atoms. It crystallizes in the triclinic $P\bar{1}$ space group.[3]

The S-oxygenation pathway of metabolic activation of thiols and thiocarbamides in the physiological environment has been extensively studied and is thought to be the predominant metabolic activation pathway for most organosulfur compounds due to the nucleophilicity of the sulfur center.[4] This implicates sulfur oxo-acids as the major metabolites of DMTU.[5–7] In the physiological environment, the formation of these sulfur oxo-acids is thought to be mediated largely by standard P450 enzymes and flavin-containing monooxygenases.[8,9] Earlier studies, and most recently our work on the oxidation of DMTU, have shown that in the presence of endogenously produced oxidants such as hydrogen peroxide, DMTU can be oxidized to produce DMAIMSA (which is also known as dimethylthiourea dioxide).[1,2]

Sulfur oxo-acids are of interest because they are considered to be physiologically more active than their parent compounds, and it is thought that most of the physiological effects associated with the parent organosulfur compounds can be ascribed to their formation.[10–13] For example, phenylthiourea, which is excreted mainly as inorganic sulfate and an organic urea residue, has been found to be extremely toxic to rats, but, surprisingly,

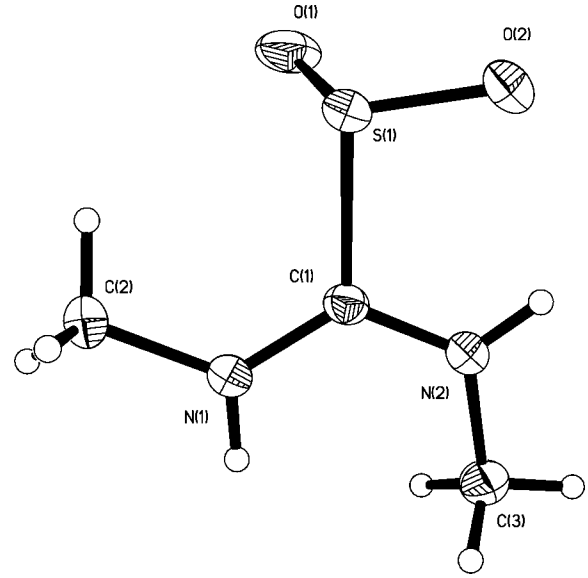

diphenylthiourea that metabolizes to a ring-cyclized product with its thione group intact is innocuous.[14–16] The subtle differences in the reactivities of these two very similar compounds can impart wildly varying physiological effects.

To evaluate the reactivities of this biologically active compound, dimethylthiourea, a well-known scavenger of reactive oxygen species,[17–20] its stable sulfur oxo-acids (the sulfinic acid, DMAIMSA, and the sulfonic acid, DMAIMSOA) were synthesized and characterized in terms of their reactivity with mild oxidants: iodine and acidified iodate.[1,3] In the IO_3^-−DMAIMSA reaction, a sigmoidal autocatalytic rate of

* Corresponding author. E-mail: rsimoyi@pdx.edu.

10.1021/jp8025013 CCC: $40.75
Published on Web 08/20/2008

formation of iodine was observed, in which acid catalyzed the formation of iodine and retarded reactions that consumed iodine. To further evaluate the reactivity of DMAIMSA, we report, in this manuscript, its oxidation by bromine and acidified bromate. The use of bromate (BrO_3^-) and bromine (Br_2), which are much stronger oxidizing agents than iodate and iodine, help to improve the understanding of the kinetics and mechanism of DMAIMSA reactions as well as the selectivity that drives the exotic dynamics that was observed in our earlier studies of the oxidation of DMAIMSA by acidic iodate. Acidic bromate and aqueous bromine are also precursors to the biologically significant oxidant, hypobromous acid, HOBr.[21]

Experimental Procedures

Materials. The following reagents were purchased and used without further purification: *N*,*N*′-dimethylthiourea, dimethylurea, hydrogen peroxide (Sigma-Aldrich), sodium bromate, perchloric acid (70%), sodium bromide (Fisher), and sodium perchlorate (Acros). Standard bromine solutions were prepared by diluting liquid bromine (Acros) under a fume hood. The bromine solutions were then standardized by iodometric titration against sodium thiosulfate in the presence of a freshly prepared starch indicator and excess acidified iodide.[22] This standardization was used to evaluate the absorptivity coefficient of 142 M^{-1} cm^{-1} for aqueous bromine at 390 nm.[23,24] DMAIMSA solutions were prepared daily, and bromine solutions, being volatile, were standardized everyday before use. DMAIMSA was synthesized by a method devised in our laboratories.[3] DMAIMSOA was prepared by reacting 0.1 mol of *N*,*N*′-dimethylthiourea with 0.3 mol equiv of hydrogen peroxide. The solution of *N*,*N*′-dimethylthiourea in 50% acetonitrile solution was stirred continuously while being cooled in an acetone/CO_2 ice bath to ensure a very slow oxidation rate that would end only at the sulfonic acid stage. The 3 equiv of H_2O_2 was added dropwise. The frozen mixture was allowed to sit until it melted and then was stirred at room temperature for 2 h. The resulting crystals were filtered and washed twice with 50% acetonitrile solution and deionized water and then air-dried in the desiccator. The crystals were recrystallized from a 50% acetonitrile solution. Doubly distilled deionized water was used for the preparation of all stock solutions.

Methods. All reactions were carried out at 25 ± 0.5 °C and a constant ionic strength of 1.0 M ($NaClO_4$). The kinetics of the two systems studied, BrO_3^-−DMAIMSA and Br_2−DMAIMSA, was monitored spectrophotometrically. The formation of aqueous bromine was followed at 390 nm while the consumption of DMAIMSA was monitored at its experimentally determined peak of 263 nm.[3] Kinetics measurements for the slower BrO_3^-−DMAIMSA system were followed on a Perkin-Elmer Lambda 25 UV−vis spectrophotometer while the faster Br_2−DMAIMSA kinetics determinations were monitored on a Hi-Tech Scientific double-mixing SF61-DX2 spectrophotometer.

Results and Discussion

Stoichiometric Determinations. Stoichiometric determinations for the BrO_3^-−DMAIMSA reaction were carried out in varying excess of acidic BrO_3^- while keeping the concentration of DMAIMSA constant. Various BrO_3^-/DMAIMSA ratios were mixed in stoppered volumetric flasks and scanned spectrophotometrically for bromine activity over a period of 24 h. At the end of the 24 h period, the excess oxidizing power of the product solution (BrO_3^- + Br_2) was determined iodometrically. The stoichiometry of the direct Br_2−DMAIMSA reaction was performed in excess bromine while varying the concentrations of DMAIMSA. The residual amount of bromine left after the reaction had gone to completion was then titrated against sodium thiosulfate as described previously. Qualitative tests and quantitative analysis for the formation of sulfate as a result of oxidation of the sulfur center in DMAIMSA in the two reaction systems were performed using barium sulfate ($BaSO_4$) precipitation.

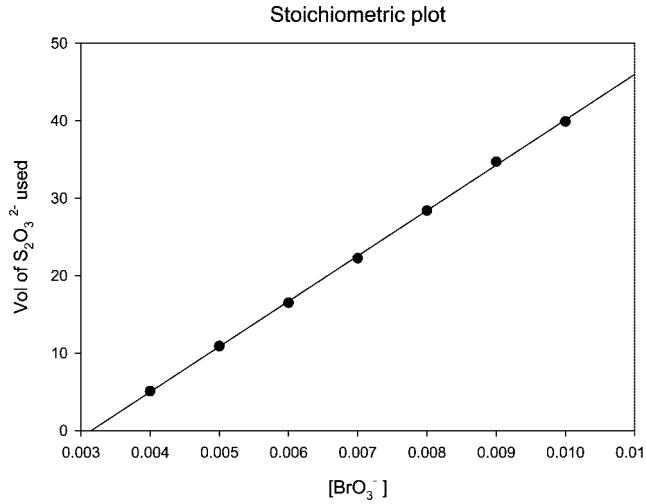

Figure 1. Stoichiometric plot generated from iodometric titration. For a fixed DMAIMSA concentration of 0.005 M, the intercept on the $[BrO_3^-]$ axis is 0.0031 M. At this point, the ratio of $[BrO_3^-]$/DMAIMSA] corresponds to that of the stoichiometry of R2.

In excess DMAIMSA conditions, the reaction of DMAIMSA with acidified bromate gave a stoichiometry of 2:3 with the major organic product being dimethylurea. The stoichiometry was confirmed as

$$2BrO_3^- + 3NHCH_3(=NCH_3)CSO_2H + 3H_2O \rightarrow 3SO_4^{2-} + 2Br^- + 3CO(NHCH_3)_2 + 6H^+ \quad (R1)$$

The stoichiometry of R1 gives the highest ratio of $[BrO_3^-]$/[DMAIMSA], *R*, possible before bromine is formed as one of the final products. The value of *R* in this case was $^2/_3$. In excess bromate conditions, when *R* exceeds $^2/_3$, the bromide product in the stoichiometry of R1 reacts with excess bromate to produce bromine[25]

$$BrO_3^- + 5Br^- + 6H^+ \rightarrow 3Br_2 + 3H_2O \quad (R2)$$

The stoichiometry of R1 also was confirmed titrimetrically. Figure 1 shows a graph of thiosulfate titer versus initial bromate concentrations for a typical series of experiments performed for stoichiometric determinations. By extrapolating to zero titer, one obtains a mol ratio of 2:3 of oxidant/reductant. This mol ratio confirms the stoichiometry of R1, with no excess bromate to effect reaction R2. As a further complementary test for the stoichiometry of R1, the gravimetric quantification of sulfate as $BaSO_4$ gave a mol ratio of 1:1 of DMAIMSA/sulfate. The amount of sulfate formed was within 96% of that expected from reaction R1. The organic urea product, dimethylurea, in R1 was confirmed by comparing the UV spectrum of the product solution to that of the reagent grade dimethylurea. In excess bromate concentrations, all bromide formed in stoichiometry R1 was oxidized to bromine by stoichiometry R2. Thus, one would expect that the overall stoichiometry in excess bromate should be a linear combination of stoichiometries R1 and R2 (5R1 + 2R2) to eliminate bromide to obtain the final stoichiometry R3

$$4BrO_3^- + 5NHCH_3(=NCH_3)CSO_2H + 3H_2O \rightarrow 5SO_4^{2-} + 2Br_2 + 5CO(NHCH_3)_2 + 6H^+ \quad (R3)$$

A confirmation of stoichiometry of R3 is evident from data obtained with varying DMAIMSA concentrations where the amount of bromine produced (measured spectrophotometrically at 390 nm) was found to be exactly 40% of the initial DMAIMSA concentrations ($0.800 > R > 0.667$). As expected, in excess bromate conditions, the titrimetric technique for quantifying the excess oxidizing power only delivered the stoichiometry of R1.

For the direct Br_2−DMAIMSA reaction, the stoichiometry as established by both titrimetric and spectrophotometric techniques was 2:1

$$2Br_2 + NHCH_3(=NCH_3)CSO_2H + 3H_2O \rightarrow SO_4^{2-} + 4Br^- + CO(NHCH_3)_2 + 6H^+ \quad (R4)$$

Reaction Dynamics. The kinetics of oxidation of DMAIMSA by bromate was followed by monitoring the formation of bromine at 390 nm and depletion of DMAIMSA at 263 nm. At 390 nm, there is little or no interference from DMAIMSA and the possible products of oxidation.[1] Figure 2 shows rapid spectral scans taken every 20 s. The final spectrum, however, was taken after 1200 s. Figure 2 shows the optical changes in the UV−vis spectrum in the course of the reaction. At the start of the reaction, there is a decrease in the absorbance of DMAIMSA at 263 nm with little or no changes at 390 nm. However, as the reaction progresses past the stoichiometry of R1 and in the presence of excess bromate, the absorbance reading at 390 nm starts to increase rapidly.

Bromate Oxidation of DMAIMSA. The dynamics of the BrO_3^-−DMAIMSA system, as monitored by the formation of bromine, in the presence of a large stoichiometric excess of bromate displayed typical clock reaction behavior.[22] Reactions were characterized by an initial quiescent induction period in which no absorbance activity was observed at 390 nm. This induction period was dependent on initial reagent concentrations. The end of the induction period is characterized by a sharp but gentle accumulation of bromine. Figure 3a shows that acid has a strong catalytic effect on the reaction. An increase in initial acid concentrations shortens the induction time noticeably. It does not alter the amount of final bromine concentrations obtained but strongly influences the rate at which this final bromine concentration is attained. A plot of induction period versus the square inverse of acid concentrations between acid concentrations of 0.1 and 0.225 M was linear (Figure 3b). A further increase in acid showed saturation, and very low acid concentrations also gave a nonlinear plot due to a tailing-off effect. This acid dependence suggests that the kinetics of the precursor reaction that leads to the measurable accumulation of bromine has a second order dependence on acid concentrations.

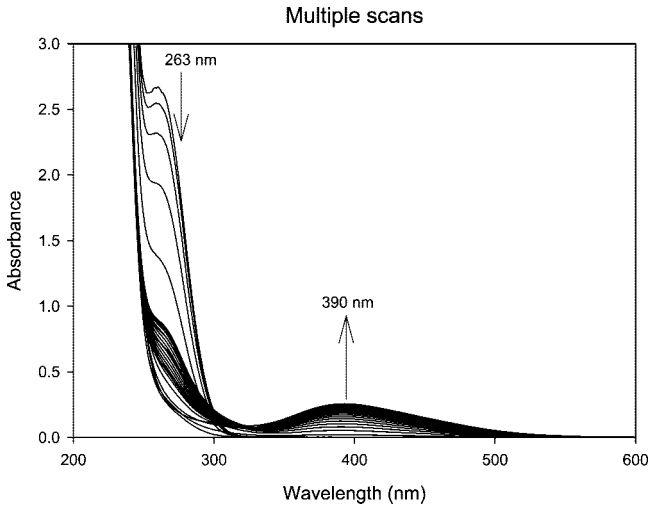

Figure 2. Rapid spectral scans taken every 20 s. Optical changes in the UV−vis spectrum for the BrO_3^-−DMAIMSA reaction are shown. Initial consumption of DMAIMSA at 263 nm with the subsequent formation of bromine at 390 nm is shown. $[DMAIMSA]_o = 0.005$ M; $[BrO_3^-]_o = 0.03$ M; and $[H^+]_o = 0.1$ M.

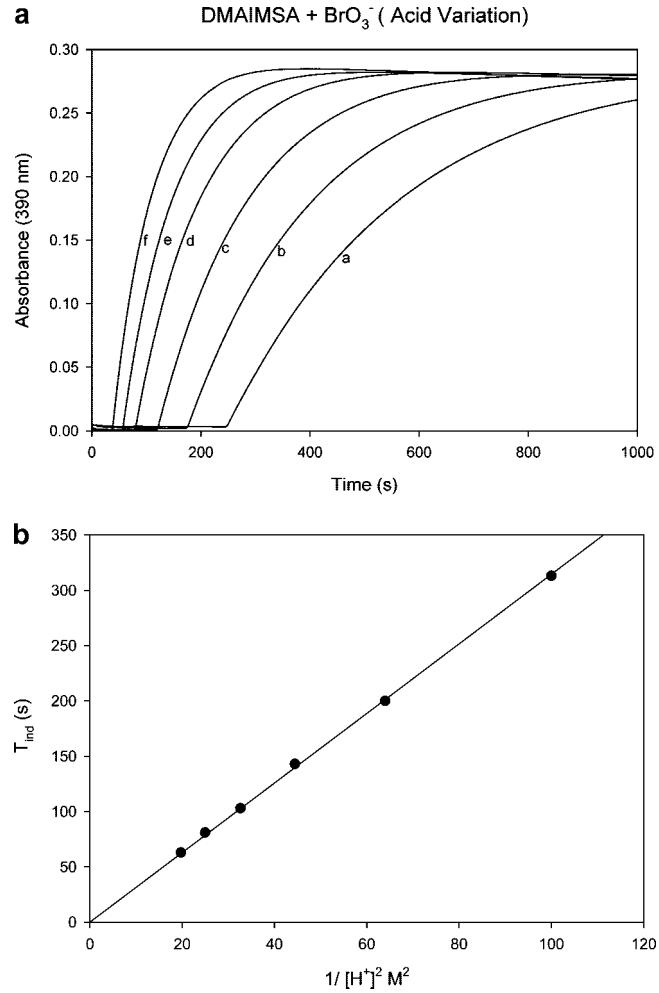

Figure 3. (a) Effect of pH on rate of formation of bromine in excess bromate conditions. An increase in $[H^+]$ concentration increases the rate of formation of bromine. $[DMAIMSA]_o = 0.005$ M; $[BrO_3^-]_o = 0.03$ M; and $[H^+]_o =$ (a) 0.100 M, (b) 0.125 M, (c) 0.150 M, (d) 0.175 M, (e) 0.200 M, and (f) 0.225 M; and $I = 1.0$ M. (b) Plot of induction time in Figure 3a vs inverse of acid concentration shows an inverse square acid dependence on induction time.

Figure 4a shows a series of experiments in which initial bromate concentrations were varied. The data show that increasing bromate concentrations enhanced the rate of reaction by shortening the length of the induction period, and for a fixed initial concentration of DMAIMSA, the final bromine concentration obtained was constant for as long as the stoichiometry of R2 was satiated. A plot of inverse of the induction time was directly proportional to initial bromate concentrations (Figure 4b). The linearity of this plot established the order of the precursor reaction (to bromine formation) with respect to bromate as unity. Figure 5a shows that in high excess of bromate ($R > 6$), the induction period becomes invariant to initial

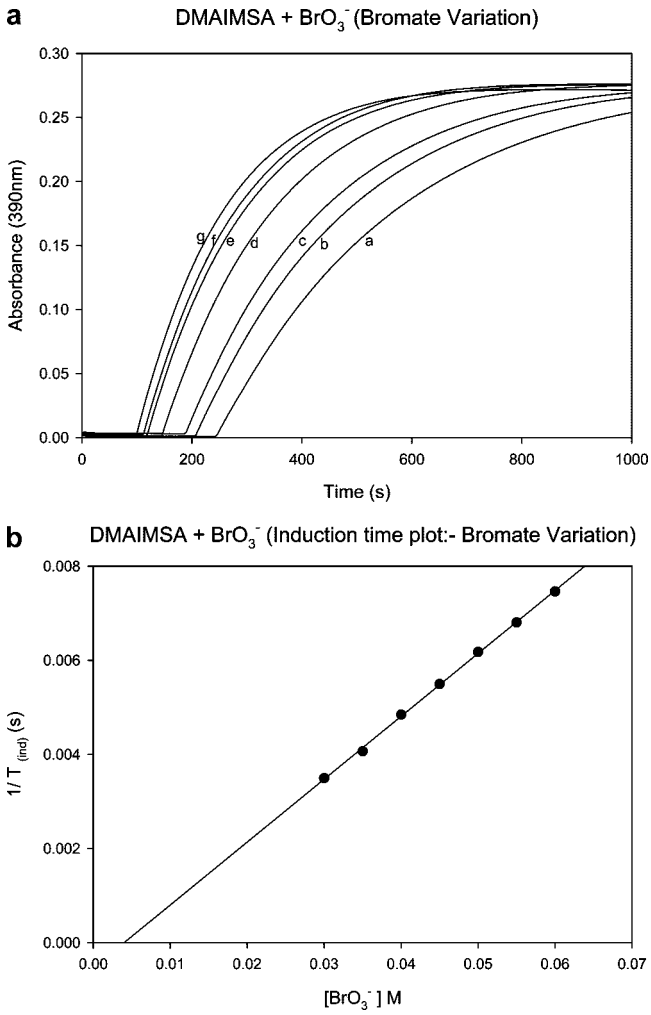

Figure 4. (a) Absorbance traces showing the effect of bromate concentrations on the rate of reaction. $[DMAIMSA]_o = 0.005$ M; $[H^+]_o = 0.10$ M; and $[BrO_3^-]_o =$ (a) 0.030 M, (b) 0.035 M, (c) 0.040 M, (d) 0.045 M, (e) 0.050 M, (f) 0.055 M, and (g) 0.060 M; and $I = 1.0$ M. (b) This plot shows that there is a direct inverse relationship between the initial concentration of bromate and the length of the induction time. Conditions are as shown in Figure 4a.

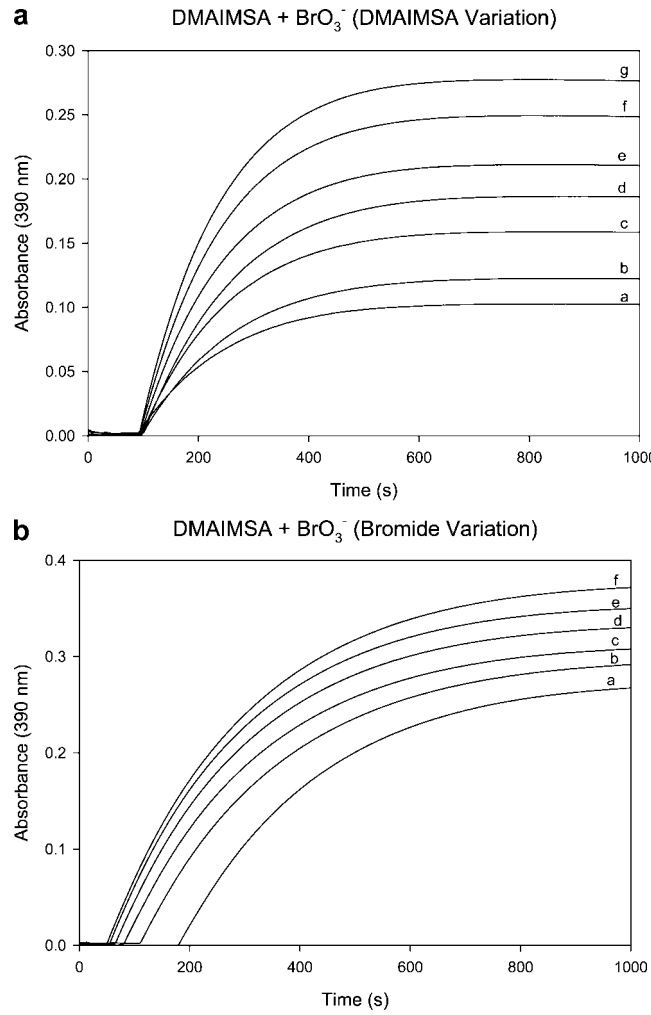

Figure 5. (a) Absorbance traces showing the effect of varying DMAIMSA concentrations on the amount of bromine formed from the BrO_3^-−DMAIMSA reaction. These traces show an increase in final amount of bromine formed as concentrations of DMAIMSA increase from trace a to trace g. This confirms that DMAIMSA is the limiting reagent in this reaction. $[DMAIMSA]_o =$ (a) 0.002 M, (b) 0.0025 M, (c) 0.003 M, (d) 0.0035 M, (e) 0.004 M, (f) 0.0045 M, and (g) 0.005 M; $[H^+]_o = 0.15$ M; $[BrO_3^-]_o = 0.03$ M; and $I = 1.0$ M. Effect of bromide on BrO_3^-−DMAIMSA. Addition of bromide (in increasing order from trace b to trace f) reduced the induction period and increased the final amount of bromine generated from the reaction. $[DMAIMSA]_o = 0.005$ M, $[H^+]_o = 0.125$ M, $[BrO_3^-]_o = 0.03$ M, and $[Br^-]_o =$ (a) 0 M, (b) 2.0×10^{-4} M, (c) 4.0×10^{-4} M, (d) 6.0×10^{-4} M, (e) 8.0×10^{-4} M, (f) 1.0×10^{-3} M, and $I = 1.0$ M.

DMAIMSA concentrations.[26] Increasing DMAIMSA concentrations only affects the rate and final amount of bromine produced according to the stoichiometry of R3. In this series of experiments, DMAIMSA is the limiting reagent. Data in Figure 5b show that bromide is also an effective catalyst in this reaction.[27] At very low concentrations of bromide (ca. 10^{-4} M), bromide ions catalyze the reaction by delivering shorter induction periods. Bromide affects not only the induction period but also the rate and final amount of bromine formed at the end of the induction period (R3). A plot of maximum bromine concentrations formed versus the initial concentration of bromide ions shows that the effect of added bromide is linear relative to the final amount of bromine (graph not shown). This linear relationship confirms that the increase in bromine concentration is based purely on the enhancement of reaction R2 by the addition of extra bromide ions to those derived from stoichiometry R1.

Data Collected at 263 nm. Figure 6a shows a sigmoidal consumption of DMAIMSA as noticed in typical autocatalytic reactions.[27] The conditions used for the generation of these data involved excess bromate concentrations with bromine formed after the requisite induction period. The traces show an initial decay in the absorbance at 263 nm followed by a sudden increase due to the formation of some species, which we surmised to be aqueous bromine and tribromide, Br_3^- (R5),[28] which has a considerable absorption coefficient at 260 nm[29]

$$Br_{2(aq)} + Br^- \rightleftharpoons Br_3^-;\ K_{eq} = 17 \qquad \text{(R5)}$$

An evaluation of the effect of acid shows that increasing acid concentrations corresponded with an increase in rate of consumption of DMAIMSA (Figure 6a) but did not increase the final absorbance of the species observed at 263 nm after complete consumption of DMAIMSA, just as in the data observed in Figure 3a. Bromate also increased the rate of consumption of DMAIMSA, and sigmoidal decay kinetics was observed for all ratios of bromate to DMAIMSA.

Data in Figure 6b show a superimposition of two sets of absorbance traces, one at 263 nm (DMAIMSA consumption) and the other at 390 nm (bromine formation), at the same initial reactant concentrations. These data show that the absorbance

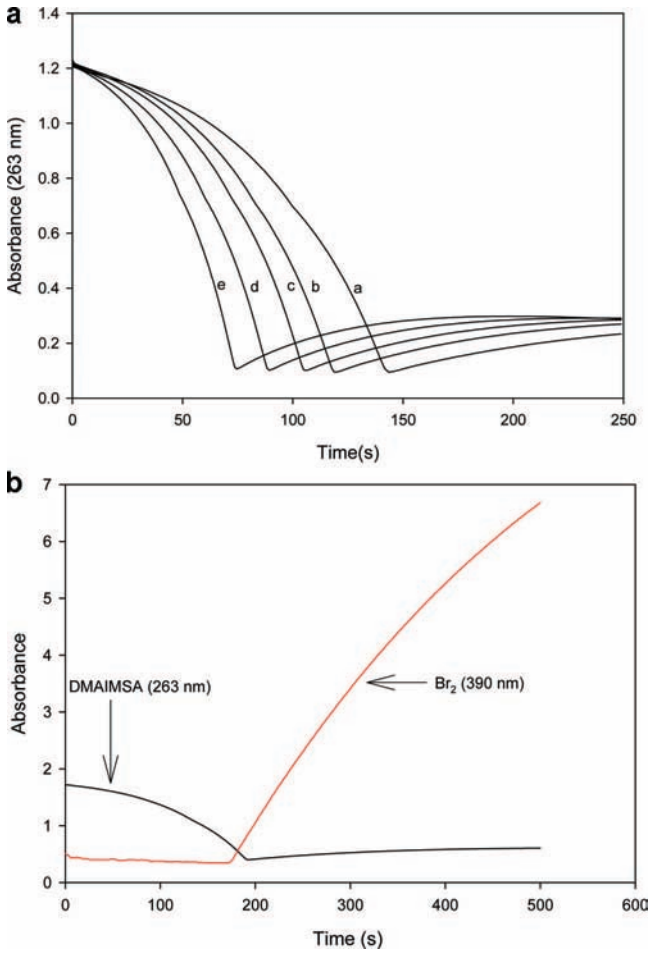

Figure 6. (a) Absorbance traces showing the effect of increasing acid concentrations on rate of consumption of DMAIMSA at 263 nm. The change in event as depicted by the sudden increase in absorbance depicts the formation of some other species, possibly tribromide, which absorbs considerably at 260 nm. $[DMAIMSA]_o = 0.0025$ M, $[BrO_3^-]_o = 0.10$ M, and $[H^+]_o =$ (a) 0.050 M, (b) 0.055 M, (c) 0.060 M, (d) 0.065 M, and (e) 0.070 M, and $I = 1.0$ M. (b) Superimposition of absorbance traces taken at 263 and 390 nm shows the accumulation of bromine only commences after DMAIMSA and possibly its transient intermediates have been completely consumed. $[DMAIMSA]_o = 0.0026$ M, $[BrO_3^-]_o = 0.10$ M, $[H^+]_o = 0.05$ M, and $I = 1.0$ M.

observed after the consumption of DMAIMSA is due to that of aqueous bromine and tribromide. According to Figure 6b, bromine does not accumulate until DMAIMSA (and possibly its transient intermediates) is consumed. This also confirms that the end of induction periods in the BrO_3^-−DMAIMSA reactions coincides with the end of absorbance activity at 263 nm and that the bromine−DMAIMSA reaction is orders of magnitude faster than the bromate−DMAIMSA reaction.

Bromine Oxidation of DMAIMSA. Data in Figure 6b suggest that the direct oxidation of DMAIMSA by bromine is much faster than its oxidation by bromate. Indeed, the direct oxidation of DMAIMSA by bromine as shown in Figure 7 confirms that this reaction is extremely fast to the extent of being diffusion-controlled. These stopped-flow traces, generated with an ensemble with 3 ms mixing time, can only catch the last 5−10% of the reaction. The major part of the reaction would be complete by the time the electronics of the stopped-flow spectrophotometer commenced recording. A conversion of absorbance reading to concentration shows that the concentrations of bromine at the start of these traces is close to the final residual bromine concentration as expected from the stoichiometry of R4. The reaction also was not slowed down sufficiently to be characterized by our stopped-flow by the addition of either bromide ions or acid.

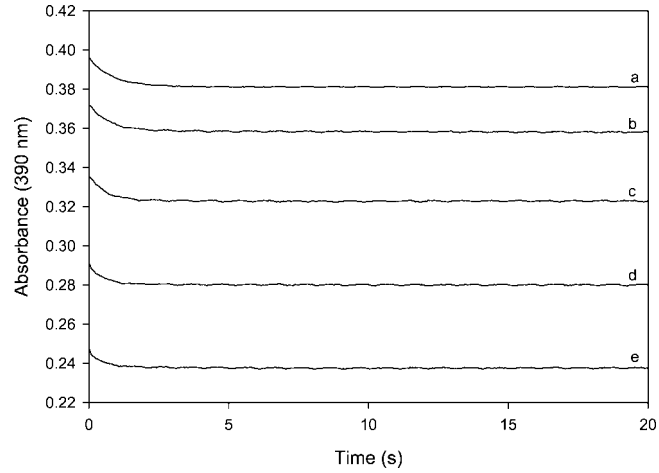

Figure 7. For a fixed concentration of bromine, the residual amount of bromine left after the Br_2−DMAIMSA reaction decreases as initial concentrations of DMAIMSA increase from trace a to trace e. $[DMAIMSA]_o =$ (a) 2.0×10^{-4} M, (b) 2.5×10^{-4} M, (c) 4.0×10^{-4} M, (d) 5.0×10^{-4} M, and (e) 7.0×10^{-4} M and $[Br_2]_o = 3.1 \times 10^{-3}$ M.

Mechanism. ***Initial Reactions.*** To propose a mechanism for the BrO_3^-−DMAIMSA reaction, three sets of possible reactions have to be considered. These reactions include oxybromine reactions, oxysulfur reactions, and oxybromine−oxysulfur reactions. The strong dependence of the induction period on the square inverse of acid concentrations (Figure 3b) and on the inverse of bromate concentrations (Figure 4b) suggests that the standard oxybromine-based kinetics dominate the initial stages of the reaction.[30,31] Since no substantial amounts of bromide ions are present at the beginning of the reaction, the major reaction during the induction period would involve the oxidation of DMAIMSA to produce bromide through the reduction of bromate. Data in Figure 6b also support the fact that bromine does not accumulate during the initial stages of the reaction. Hence, in the absence of bromide and bromine at the start of the reaction, the first step should involve the direct reaction of acidified bromate and DMAIMSA.

$$BrO_3^- + H^+ \rightleftharpoons HBrO_3 \quad \text{(R6)}$$

$$HBrO_3 + NHCH_3(=NCH_3)CSO_2H + H^+ \rightarrow NHCH_3(=NCH_3)CSO_3H + H^+ + HBrO_2 \quad \text{(R7)}$$

R7 can be written as a bimolecular reaction with acidified bromic acid as the electrophilic species, $H_2BrO_3^+$. Several previous workers in bromate chemistry have postulated this $H_2BrO_3^+$ species to justify the observed second order dependence on acid in all bromate-based oxidations in highly acidic media.[32] A mechanism, written in the form of R7, in which the second proton would be used to dissociate the complex formed between bromic acid and DMAIMSA would be kinetically indistinguishable from one involving $H_2BrO_3^+$ since they would both deliver a reaction order of 2 with respect to acid concentrations.

Bromous acid ($HBrO_2$),[33] which represents the first oxybromine species, can be further reduced, through a series of two-electron cascades, to Br^-.[34]

$$HBrO_2 + 2H^+ + 2e^- \rightleftharpoons HOBr + H_2O \quad (R8)$$

$$HOBr + H^+ + 2e^- \rightleftharpoons Br^- + H_2O \quad (R9)$$

The two-electron reductants in R8 and R9 can be DMAIMSA, its oxidative metabolites, or bromide (if it has accumulated sufficiently enough). The production of bromide in R9 then initiates the most important oxyhalogen reaction: the reaction of bromate and bromide, which produces more of the reactive oxybromine species, $HBrO_2$ and HOBr.[27,35]

$$BrO_3^- + Br^- + 2H^+ \rightarrow HBrO_2 + HOBr \quad (R10)$$

R10, is, of course, a composite reaction that involves several steps but has been studied sufficiently enough such that the forward and reverse apparent rate constants have been accurately determined as a fourth order reaction in the forward reaction. $HBrO_2$ is unstable with respect to HOBr in the presence of Br^- ions.[31] It will readily disproportionate to produce hypobromous acid (R11)

$$HBrO_2 + Br^- + H^+ \rightarrow 2HOBr \quad (R11)$$

HOBr is such a strong oxidant and reactive species that it will be rapidly reduced in a subsequent two-electron reduction to produce more bromide (reaction R9). The well-known rapid rate of reaction R11[33] can allow us to generate a plausible mechanism that does not involve $HBrO_2$ as a major oxidizing species. The initial stages of the reaction, culminating with the observed sigmoidal decay consumption of DMAIMSA, involve the accumulation of bromide. One mol of bromide in reaction R10 ultimately produces 2 mol of bromide from the subsequent reduction of $HBrO_2$ and HOBr.

If R9 and R11 are both faster than R7 and R10, it is expected that a combination of these reactions 3R9 + R10 + R11 will be autocatalytic in bromide production:

$$BrO_3^- + 2Br^- + 6H^+ + 6e^- \rightarrow 3Br^- + 3H_2O \quad (R12)$$

There have been suggestions that the bromate species is extremely inert and that bromate oxidations are initiated by trace amounts of bromide ions that are contained in most bromate solutions, irrespective of how pure they are. These trace bromide ions would initiate R10, delivering the same autocatalytic build-up of bromide ions and offering the same sigmoidal decay kinetics. While the mechanistic basis of such an assertion is plausible, we found that these trace bromide concentrations are insufficient to support the observed rate of reaction. Using a specific bromide electrode, a standard 0.02 M sodium bromate solution made from reagent grade sodium bromate (Fisher) contains $\sim 5.0 \times 10^{-6}$ M sodium bromide as an impurity.[27] A rough calculation, using the well-known kinetics constants for oxybromine reactions, produces reaction rates and induction periods an order of magnitude slower that our experimental observations. Although this pathway exists, it is not the sole pathway by which bromide is autocatalytically produced.

Formation of Bromine. The major pathway to the formation of bromine involves the reaction of HOBr with bromide ions[36]

$$HOBr + Br^- + H^+ \rightleftharpoons Br_2 + H_2O \quad (R13)$$

Since the direct oxidation of DMAIMSA by bromine is fast (Figure 7), bromine formed in R13 should not accumulate, and the induction period should persist until all DMAIMSA and its metabolites in the reaction medium are consumed. The rate of formation of bromine at the end of the induction period, therefore, depends on available excess bromate, bromide, and acid concentrations (as observed in Figures 4a, 5b, and 3a, respectively). The final concentration of bromine produced, as well as the rate of its formation, was found to be directly proportional to the concentration of bromide ions produced in the stoichiometry of R1 and thus was directly proportional to the initial concentration of DMAIMSA in excess bromate conditions (Figure 5a).

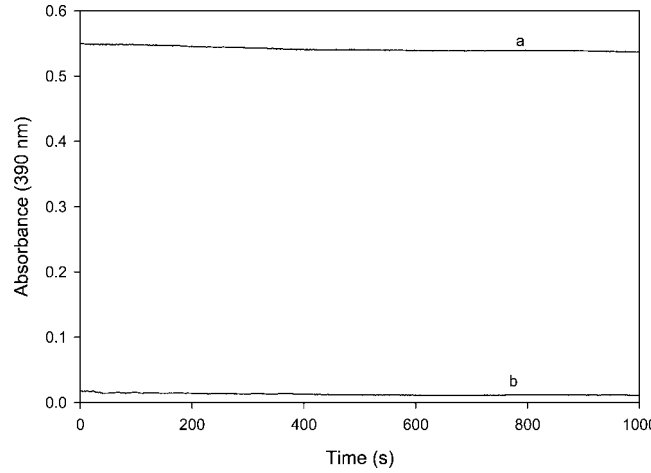

Figure 8. Traces showing the difference in direct oxidation of DMAIMSA and DMAIMSOA by bromine. The oxidation of DMAIMSOA is relatively inert (trace a) when compared to that of DMAIMSA (trace b). $[Br_2]_o = 3.6 \times 10^{-3}$ M (a) and $[DMAIMSOA]_o = 0.05$ M and (b) $[DMAIMSA]_o = 0.03$ M.

Oxidation of DMAIMSA. The oxidation of DMAIMSA can be effected by the various oxybromine and bromine species produced in solution. By invoking rapid reaction R11, we can assume that DMAIMSA is oxidized predominantly by HOBr and Br_2(aq). The autocatalytic oxidation rate of DMAIMSA is directly linked to the autocatalytic bromide production (composite reaction R12), which is a prerequisite for the production of the reactive oxidizing species, HOBr and Br_2(aq). Both of these oxidizing species are two-electron oxidants, and it would be reasonable to assume that they should both oxidize DMAIMSA to the corresponding sulfonic acid, DMAIMSOA, as in R14:

$$Br_2/HOBr + NHCH_3(=NCH_3)CSO_2H\ (+ H_2O) \rightarrow NHCH_3(=NCH_3)CSO_3H + 2Br^-/Br^- + 2H^+/H^+ \quad (R14)$$

Further oxidation of $NHCH_3(=NCH_3)CSO_3H$ should yield the end product, sulfate, and dimethylurea

$$NHCH_3(=NCH_3)CSO_2H + 2H_2O \rightarrow CO(NHCH_3)_2 + SO_4^{2-} + 4H^+ + 2e^- \quad (R15)$$

We, however, synthesized DMAIMSOA specifically for the purposes of proving the existence of and determining the rate of R14 and R15. The direct oxidation of DMAIMSOA by bromine was very slow even in conditions of excess bromine, while that of DMAIMSA was extremely fast at almost identical conditions (see Figure 8). Figure 8 shows that DMAIMSOA is inert to oxidation and that aqueous bromine solutions maintained their titer even after 1000 s while DMAIMSA was rapidly oxidized by aqueous bromine within milliseconds. DMAIMSOA solutions, left overnight (aged), showed a little more reactivity than freshly prepared solutions. In acidic media, however, even aged DMAIMSOA solutions were inert to further oxidation to DMU.[1,37] The observed reactivity with aged solutions suggests that DMAIMSOA only further reacts after an initial irreversible

slow hydrolysis to yield DMU and bisulfite (R16), with further oxidation of bisulfite by either Br_2 and HOBr (R17) being so fast to the extent of diffusion-controlled rates[38]

$$NHCH_3(=NCH_3)CSO_3H + H_2O \rightarrow CO(NHCH_3)_2 + H^+ + HSO_3^- \quad (R16)$$

$$HOBr + HSO_3^- \rightarrow Br^- + HSO_4^- + H^+ \quad (R17)$$

One also can assume that an initial hydrolysis of DMAIMSA to yield the sulfoxylate anion (R18) could be the major oxidation pathway that avoids passing through DMAIMSOA

$$NHCH_3(=NCH_3)CSO_2H + H_2O \rightarrow CO(NHCH_3)_2 + H^+ + HSO_2^- \quad (R18)$$

The sulfoxylate anion is known to produce the sulfoxylate anion radical in aerobic conditions, which is a precursor to dithionite[39]

$$HSO_2^- + O_2 \rightarrow SO_2^{\cdot -} + H^+ + O_2^{\cdot -} \quad (R19)$$

$$2SO_2^{\cdot -} \rightleftharpoons S_2O_4^{2-} \quad (R20)$$

Dithionite is well-known by its signature absorbance at 315 nm. Some of our previous work showed the formation of dithionite in alkaline aerobic conditions of DMAIMSA.[3,39] No dithionite was detected at the acidic conditions used for the present study, suggesting that R18 is a minor or negligible pathway. Acidic solutions of DMAIMSA maintained their titer (just like DMAIMSOA) for hours, while alkaline DMAIMSA solutions rapidly decomposed.[1] The rapid rate of oxidation of DMAIMSA excludes the slow hydrolysis R18.

One remarkable feature of the C−S bond of DMAIMSA, at 0.188 nm,[1,3] is that it is much longer than the theoretical prediction[40] of 0.179 nm if one just adds the covalent radii of the two atoms. The same feature was observed in other aminosulfinic acids.[40] The length of this bond suggests that it is very weak and easily cleaved by an attack on the positively disposed carbon atom by even the weakest mucleophiles such as water. The weakness of this bond has been used in the textile industry since the oxidation of aminoiminomethanesulfinic acid is used as a radical species generator after homolytic cleavage of the C−S bond. It also was used in the synthesis of guanidines by displacing the sulfur leaving group and forming a C=N bond.[41] Hence, we postulate that the major oxidation pathway of DMAIMSA is its direct oxidation straight to DMU and bisulfite, without passing through DMAIMSOA. The weakness of the C−S bond makes this possible.

$$NHCH_3(=NCH_3)CSO_2H + 2H_2O + Br_2(aq) \rightarrow CO(NHCH_3)_2 + 3H^+ + HSO_3^- + 2Br^- \quad (R21)$$

Further oxidation of the bisulfite should be facile, as in R17.

$$Br_2(aq) + HSO_3^- + H_2O \rightarrow HSO_4^- + 2Br^- + 2H^+ \quad (R22)$$

The diffusion-controlled rate of reaction in the bromine−DMAIMSA reaction, which our stopped-flow spectrophotometer could not characterize, is R21 and not the hydrolysis of R18 followed by oxidation of the sulfoxylate anion nor its oxidation to DMAIMSOA (R14). We estimate, from the direct oxidation of DMAIMSA, that the bimolecular rate constant for its oxidation by aqueous bromine has a lower limit of $5.5 \pm 1.5 \times 10^4$ M^{-1} s^{-1}. The analogous reaction R21 of oxidation of DMAIMSA by HOBr, which in this case is an oxygen transfer, should be equally rapid

$$NHCH_3(=NCH_3)CSO_2H + HOBr + H_2O \rightarrow CO(NHCH_3)_2 + HSO_3^- + 2H^+ + Br^- \quad (R23)$$

TABLE 1: Model Used for Computer Simulations

number	reaction	k_f; k_r
M1	$BrO_3^- + 2H^+ + Br^- \rightleftharpoons HBrO_2 + HOBr$	2.1; 1.0×10^4
M2	$HBrO_2 + Br^- + H^+ \rightleftharpoons 2HOBr$	2.0×10^9; 2.0×10^{-5}
M3	$HOBr + Br^- + H^+ \rightleftharpoons Br_2 + H_2O$	8.9×10^9; 110
M4	$2HBrO_2 \rightleftharpoons BrO_3^- + HOBr + H^+$	4.0×10^7; 2.0×10^{-10}
M5	$H^+ + BrO_3^- \rightleftharpoons HBrO_3$	1.00×10^8; 4.00×10^7
M6	$Br_2 + Br^- \rightleftharpoons Br_3^-$	1.50×10^9; 8.8×10^7
M7	$HBrO_3 + DMAIMSA + H^+ + (H_2O) \rightarrow HBrO_2 + DMU + HSO_3^- + H^+$	1.15×10^2
M8	$HBrO_2 + DMAIMSA + (H_2O) \rightarrow HOBr + DMU + HSO_3^- + H^+$	1.0×10^3
M9	$HOBr + DMAIMSA + H_2O \rightarrow Br^- + DMU + HSO_3^- + 2H^+$	5.0×10^6
M10	$Br_2 + DMAIMSA + H_2O \rightarrow Br^- + DMU + HSO_3^- + 2H^+$	1.0×10^5
M11	$DMAIMSA + H_2O \rightarrow DMU + HSO_2^- + H^+$	2.0×10^{-2}
M12	$Br_2 + HSO_2^- + H_2O \rightarrow 2Br^- + HSO_3^- + 2H^+$	2.5×10^6
M13	$HOBr + HSO_2^- \rightarrow Br^- + HSO_3^- + H^+$	5.0×10^6
M14	$Br_2 + HSO_3^- + H_2O \rightarrow 2Br^- + SO_4^{2-} + 3H^+$	1.0×10^5
M15	$HOBr + HSO_3^- \rightarrow Br^- + SO_4^{2-} + 2H^+$	1.0×10^5

Computer Simulations. The mechanism used for simulations was not exhaustive and considered only those reactions that were relevant in the highly acidic medium employed for the series of experiments profiled in this manuscript. A very different mechanism would be more relevant in basic media, but this basic medium would not support bromate oxidations that are only viable in acidic media. The mechanism profiled in Table 1 can be broken down into three distinct groups. The first group, M1−M6, is the group of standard oxybromine and bromine reactions whose rate constants and general kinetics parameters are known from literature values.[30,31] The second group, M7−M10, involves the initiation and oxidation reactions of the substrate by oxybromine species. These reactions are considered to be irreversible. The last group of reactions, M12−M15, represents the rapid oxidations of sulfur leaving groups by aqueous bromine and hypobromous acid. One lone reaction is M11, which represents the hydrolysis of DMAIMSA to the sulfoxylate anion. This was included because DMAIMSA is known to give dithionite in aerobic solutions and the precursor to dithionite is the SO_2^{2-} leaving group in M11.[1]

Table 2 shows a set of reactions that were excluded from the mechanism based on experimental data. M16 is a two-electron oxidation of DMAIMSA that yields DMAIMSOA. This reaction was excluded because the DMAIMSOA we synthesized showed no reactivity and was extremely inert in acidic solutions. The subsequent reaction M17 is a hydrolysis reaction comparable to M11, yielding bisulfite. This reaction is facile in basic

TABLE 2: Reactions Excluded from the Simulations Mechanism

number	reaction	k_f; k_r
M16	$HBrO_3 + DMAIMSA + H^+ \rightarrow HBrO_2 + DMAIMSOA + H^+$	
M17	$DMAIMSOA + H_2O \rightarrow DMU + HSO_3^- + H^+$	2.0×10^{-2}
M18	$H^+ + DMAIMSA \rightleftharpoons [ZW\text{-}DMAIMSA]^+$	fast; both ways
M19	$H^+ + DMAIMSOA \rightleftharpoons [ZW\text{-}DMAIMSOA]^+$	fast; both ways

environments and would be insignificant in the environment of interest in this manuscript. Even though M16 and M17 could have been included in Table 1, we would have had to give them vanishingly low rate constants. Reactions M18 and M19 are the reactions that would have been utilized to explain the inertness of both DMAIMSA and DMAIMSOA in acidic environments. They involve the protonation of zwitterions in acidic medium, rendering them inert to electrophilic attack. The equilibrium constants used for these reactions would not have any thermodynamic significance. They would only be useful to quantify the effect of acid in stabilizing the DMAIMSA and DMAIMSOA zwitterions in acidic media. Since they are protolytic reactions, they are very fast (in both directions) and would stiffen and slow down the simulations considerably, without any improvement in the subsequent precision of the calculations.

Simulations could be simplified by assuming that acid concentrations were buffered throughout the lifetime of the reaction. Acid, in all experimental data shown in this manuscript, was in overwhelming excess and did not vary much during the course of the reaction. Thus, effectively, reactions M2 and M3 were essentially bimolecular, with apparent rate constants that involved a product standard rate constants multiplied by the (constant) acid concentrations. Even without this stipulation, simulating the temporal variation of acid concentrations showed no activity. The buffering of acid concentrations only served to simplify the model.

There were not that many rate constants that could be estimated or varied. For example, the kinetics parameters used in reactions M1−M4 were fixed by literature values. Reaction M5, being a protolytic reaction, was assumed to be diffusion-controlled. The forward and reverse rate constants adopted, however, did not alter the simulations results for as long as they were fast (in both directions). The important parameter for the reaction was the acid dissociation constant adopted for bromic acid. There have been several studies on the acid dissociation constant of bromic acid, with widely varying values given.[32] We estimate that bromic acid concentrations become significant in pH conditions lower than 2, which encompasses all the experimental results shown here. We adopted an acid dissociation constant for bromic acid as 2.5, and this controlled the ratio of the forward and reverse rate constants for reaction M5. Raman spectroscopy data gave an association rate constant between H^+ and BrO_3^- of 2.6×10^{11} M^{-1} s^{-1}.[42] We could use a lower value (computationally less stiff) for as long as the pK_a value was maintained. Oxidation rates of bisulfite by oxyhalogens were studied by Margerum et al., and all rate constants used for reactions M12−M15 were estimated from their work.[38,43,44] However, any values, for as long as they were fast, were acceptable for our model. In the adopted highly acidic conditions, very little hydrolysis of DMAIMSA occurred as in M11, and a very low rate constant was adopted. Further research is needed for the derivation of a reasonable hydrolysis rate constant for M11, which is known to be heavily dependent on pH. The most important reaction in the model was the initiation reaction M7. The adopted value controlled the induction period as well as the rate of bromine formation after the induction period. Reaction M6 was added to account for possible retardation of the reaction by the addition of bromide to form a relatively inert electrolyte, Br_3^-. The adopted rate constants were derived from the work of Ruasse et al.[28] Since no retardation was observed by the addition of bromide, we surmise that the reaction of tribromide is equally fast, and so reaction M6 was deactivated for the final simulations results shown in Figure 9a,b.

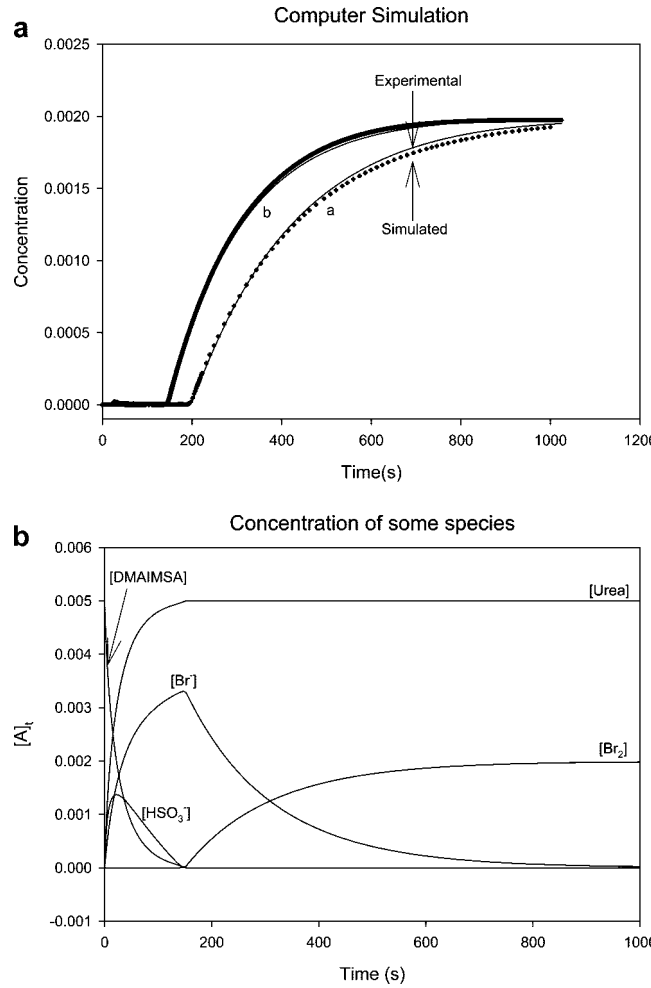

Figure 9. (a) Computer modeling using the reaction mechanism shown in Table 1. Reaction conditions are the same as those in Figure 3a (traces b and c). $[DMAIMSA]_o = 0.005$ M, $[BrO_3^-]_o = 0.03$ M, and $[H^+]_o =$ (a) 0.125 M and (b) 0.150 M. (b) Modeling of some of the species involved in the DMAIMSA−bromate reaction. The concentration of these species could not be followed experimentally. Conditions are the same as those in Figure 9a. This model predicts that the consumption of DMAIMSA and its possible intermediate is necessary before bromine begins to accumulate. Bromide concentration rises to the maximum before it begins to decrease, and the rate of bromide consumption seems to be proportional to the rate of bromine formation from bromate.

Figure 9a shows a good fit of the simulations to experimental data using the simplified mechanism shown in Table 1. This mechanism was able to simulate the induction period and bromine formation. The model also satisfactorily reproduces the effect of acid on induction period and rate of formation of bromine at the end of the induction period as shown in Figure

3a (traces b and c). Figure 9b shows the concentration variations of some intermediate species that could not be experimentally determined.

Conclusion

Even though acidic bromate and bromine are very strong oxidizing agents, they do not oxidize DMAIMSA through DMAIMSOA. DMAIMSOA is very stable to further oxidation, even in the presence of these strong oxidants. Since the stoichiometric equivalent was attained rapidly (within 20 s), it is reasonable to conclude that the cleavage of the C−S bond occurs at the sulfinic acid stage. This assertion is also verified by the abnormally long C−S bond in DMAIMSA.

Acknowledgment. This work was supported by Research Grant 0614924 from the National Science Foundation.

References and Notes

(1) Otoikhian, A.; Simoyi, R. H.; Petersen, J. L. *Chem. Res. Toxicol.* **2005**, *18*, 1167–1177.
(2) Curtis, W. E.; Muldrow, M. E.; Parker, N. B.; Barkley, R.; Linas, S. L.; Repine, J. E. *Proc. Natl. Acad. Sci. U.S.A.* **1988**, *85*, 3422–3425.
(3) Ojo, J. F.; Petersen, J. L.; Otoikhian, A.; Simoyi, R. H. *Can. J. Chem.* **2006**, *84*, 825–830.
(4) Del Corso, A.; Cappiello, M.; Mura, U. *Int. J. Biochem.* **1994**, *26*, 745–750.
(5) Chigwada, T. R.; Chikwana, E.; Simoyi, R. H. *J. Phys. Chem. A* **2005**, *109*, 1081–1093.
(6) Chigwada, T. R.; Simoyi, R. H. *J. Phys. Chem. A* **2005**, *109*, 1094–1104.
(7) Henderson, M. C.; Krueger, S. K.; Stevens, J. F.; Williams, D. E. *Chem. Res. Toxicol.* **2004**, *17*, 633–640.
(8) Madan, A.; Parkinson, A.; Faiman, M. D. *Biochem. Pharmacol.* **1993**, *46*, 2291–2297.
(9) Guo, W. X.; Poulsen, L. L.; Ziegler, D. M. *Biochem. Pharmacol.* **1992**, *44*, 2029–2037.
(10) Neal, R. A. *Reviews in Biological Toxicology*; Elsevier: Amsterdam, 1980; pp 131−171.
(11) Neal, R. A.; Kamataki, T.; Hunter, A. L.; Catignani, G. *Microsome and Drug Oxidations*; Pergamon: New York, 1977; pp 467−475.
(12) Neal, R. A.; Halpert, J. *Annu. Rev. Pharmacol. Toxicol.* **1982**, *22*, 321–339.
(13) Svarovsky, S. A.; Simoyi, R. H.; Makarov, S. V. *J. Phys. Chem. B* **2001**, *105*, 12634–12643.
(14) Kim, S. G.; Kim, H. J.; Yang, C. H. *Chem. Biol. Interact.* **1999**, *117*, 117–134.
(15) Scott, A. M.; Powell, G. M.; Upshall, D. G.; Curtis, C. G. *Environ. Health Perspect.* **1990**, *85*, 43–50.
(16) Smith, R. L.; Williams, R. T. *J. Med. Pharm. Chem.* **1961**, *4*, 97–107.
(17) Linas, S. L.; Shanley, P. F.; White, C. W.; Parker, N. P.; Repine, J. E. *Am. J. Physiol.* **1987**, *253*, 692–701.
(18) Parker, N. B.; Berger, E. M.; Curtis, W. E.; Muldrow, M. E.; Linas, S. L.; Repine, J. E. *J. Free Radical Biol. Med.* **1985**, *1*, 415–419.
(19) Toth, K. M.; Harlan, J. M.; Beehler, C. J.; Berger, E. M.; Parker, N. B.; Linas, S. L.; Repine, J. E. *Free Radical Biol. Med.* **1989**, *6*, 457–466.
(20) Wasil, M.; Halliwell, B.; Grootveld, M.; Moorhouse, C. P.; Hutchison, D. C.; Baum, H. *Biochem. J.* **1987**, *243*, 867–870.
(21) Thomas, E. L.; Bozeman, P. M.; Jefferson, M. M.; King, C. C. *J. Biol. Chem.* **1995**, *270*, 2906–2913.
(22) Darkwa, J.; Olojo, R.; Olagunju, O.; Otoikhian, A.; Simoyi, R. *J. Phys. Chem. A* **2003**, *107*, 9834–9845.
(23) Epstein, I. R.; Kustin, K.; Simoyi, R. H. *J. Phys. Chem.* **1992**, *96*, 6326–6331.
(24) Simoyi, R. H.; Epstein, I. R.; Kustin, I. *J. Phys. Chem.* **1994**, *98*, 551–557.
(25) Lopez-Cueto, G.; Ostra, M.; Ubide, C. *Anal. Chim. Acta* **2001**, *445*, 117–126.
(26) Jonnalagadda, S. B.; Chinake, C. R.; Simoyi, R. H. *J. Phys. Chem.* **1995**, *99*, 10231–10236.
(27) Chinake, C. R.; Simoyi, R. H.; Jonnalagadda, S. B. *J. Phys. Chem.* **1994**, *98*, 545–550.
(28) Ruasse, M.-F.; Aubard, J.; Galland, B.; Adenir, A. *J. Phys. Chem.* **1986**, *90*, 4382–4388.
(29) Chikwana, E.; Otoikhian, A.; Simoyi, R. H. *J. Phys. Chem. A* **2004**, *108*, 11591–11599.
(30) Noyes, R. M.; Field, R. J.; Thompson, R. C. *J. Am. Chem. Soc.* **1971**, *93*, 7315–7316.
(31) Noyes, R. M. *J. Am. Chem. Soc.* **1980**, *102*, 4644–4649.
(32) Sortes, C. E.; Faria, R. B. *J. Braz. Chem. Soc.* **2001**, *12*, 775–779.
(33) Faria, R. D.; Epstein, I. R.; Kustin, K. *J. Phys. Chem.* **1994**, *98*, 1363–1367.
(34) Madhiri, N.; Olojo, R.; Simoyi, R. H. *Phys. Chem. Chem. Phys.* **2003**, *5*, 4149–4156.
(35) Noyes, R. M. *J. Am. Chem. Soc.* **1980**, *102*, 4644–4649.
(36) Kustin, K.; Eigen, M. *J. Am. Chem. Soc.* **1962**, *84*, 1355–1359.
(37) Makarov, S. V.; Mundoma, C.; Penn, J. H.; Svarovsky, S. A.; Simoyi, R. H. *J. Phys. Chem. A* **1998**, *102*, 6786–6792.
(38) Yiin, B. S.; Margerum, D. W. *Inorg. Chem.* **1989**, *29*, 1559–1564.
(39) Svarovsky, S. A.; Simoyi, R. H.; Makarov, S. V. *J. Chem. Soc., Dalton Trans.* **2000**, 511–514.
(40) Makarov, S. V.; Mundoma, C.; Penn, J. H.; Petersen, J. L.; Svarovsky, S. A.; Simoyi, R. H. *Inorg. Chim. Acta* **1999**, *286*, 149–154.
(41) Maryanoff, C. A.; Stanzione, R. C.; Plampin, J. N.; Mills, J. E. *J. Org. Chem.* **1986**, *51*, 1882–1884.
(42) Alves, W. A.; Tellez, C. A.; Sala, O.; Santos, P. S.; Faria, R. B. *J. Raman Spectrosc.* **2001**, *32*, 1032–1036.
(43) Hartz, K. E. H.; Nicoson, J. S.; Wang, L.; Margerum, D. W. *Abstr. Pap. Am. Chem. Soc.* **2002**, *224*, 747.
(44) Hartz, K. E. H.; Nicoson, J. S.; Wang, L.; Margerum, D. W. *Inorg. Chem.* **2003**, *42*, 78–87.

JP8025013